

Research paper

Study of energy scheduling and optimal cost management of a new structure CCHP system: A case study supplying energy for a chemical enterprise in Jiangsu Province

Jie Ji^{a,*}, Jingxin Qin^a, Rundong Ji^b, Hui Huang^a, Fucheng Wang^a, Muhammad Shahzad Nazir^a, Mengxiong Zhou^a, Yaodong Wang^c

^a Huaiyin institute of technology, Huaiyin Jiangsu 223002, China

^b Jiangsu Huashui Engineering Detection & Consulting Co.Ltd, China

^c Durham Energy Institute, Durham University, United Kingdom

ARTICLE INFO

Article history:

Received 2 August 2022

Received in revised form 25 September 2022

Accepted 22 October 2022

Available online xxxx

Keywords:

CCHP system

Chemical enterprises

Energy scheduling

Whale optimization algorithm

ABSTRACT

A new structure combined cooling, heating and power (CCHP) system integrating green power applying a control strategy based on a improved whale optimization algorithm is proposed in this paper. This paper fully considers the high energy demand and a large amount of waste heat in chemical enterprises. By absorbing chemical waste heating (mainly from chemical wastewater), coupling wind and photovoltaic equipment, adding cooling, heating, and electricity storage equipment, combined with an energy scheduling strategy, and an efficient CCHP energy system for the target enterprise is realized. The improved whale optimization algorithm is used to optimize cost management. The results show that after the optimization scheduling with the improved whale optimization algorithm, the CCHP system meets the energy demand with higher efficiency at a lower cost. In winter and summer, heat pump recycling chemical wastewater provides 15.4%–57.9% and 11.5%–62.9% of the heating load of the heating network. Meanwhile, the lithium bromide refrigerator in the cooling-net equipment provides an average cooling load of 6.25–58.4% and 7.01–16.64%. Finally, the improved whale optimization algorithm reduces the total cost by 2.4 % and 2.17 %.

© 2022 The Author(s). Published by Elsevier Ltd. This is an open access article under the CC BY-NC-ND license (<http://creativecommons.org/licenses/by-nc-nd/4.0/>).

1. Introduction

Nowadays, the world lacks resources, and a variety of non-renewable energy resources such as coal, oil, natural gas, and other fossil fuels are diminishing. Using fossil fuels to supply energy produces many greenhouse gases (GHG), and other harmful gases are generated (Xu et al., 2022). China is implementing more stringent environmental policies to reduce carbon emissions (Yin, 2021). Therefore, Energy and environmental issues have become the most critical issues for human development.

CCHP (Combined Cooling Heating and Power) is one of the critical forms of distributed energy systems. As an energy system supplying electricity, heating, and cooling, the CCHP system has attracted wide attention due to its high energy utilization efficiency, safety, reliability, and environmental protection (Jiaxiu et al., 2022).

Foreign countries, such as Japan, America, and Germany, have studied and applied the CCHP system for a long time (Linlin

and Qinrong, 2020). Because the CCHP system is different from the traditional centralized energy supply system (power plant as the core, long-distance transmission structure), which can supply three kinds of energy simultaneously, it can provide cooling, heating, and electricity simultaneously. Applying CCHP systems to give power is proven beneficial in improving energy supply efficiency and air quality (Xuntao and Gaoyan, 2020). However, as a kind of distributed energy supply system, its use is limited and generally only used in independent places such as buildings or industrial parks (Xinrou, 2022).

Many chemical processes are exothermic reactions, and the discharged chemical wastewater is also full of energy. CCHP system is a good choice as an energy supplier for chemical enterprises. Currently, most research and applications of CCHP systems are concentrated in commercial buildings (Mingzhe et al., 2022; Liang et al., 2021; Tooryan et al., 2022). There are few cases applying the CCHP system to the energy supply for chemical enterprises in China, and few people have conducted similar simulations or experiments in this area.

Take a case to illustrate the application of the existing CCHP system to chemical enterprises. The research shows that Shouyang (2022) has recently applied the CCHP system to the

* Corresponding author.

E-mail address: dahuoxun@hotmail.com (J. Ji).

Nomenclature

$a_{BO,1}$	The gas inlet rate coefficient of the heat boiler in operation
$a_{GT,1}$	The gas inlet rate coefficient of the gas turbine in operation
$a_{HP,1}$	The water inlet speed coefficient of the heat pump operation
$a_{LBR,1}$	Gas inlet coefficient of lithium bromide refrigerator
$a_{LBR,2}$	Water inlet coefficient of lithium bromide refrigerator
BO	Heat boiler
C_{pow}	The cost of buying electricity (¥)
C_{sell}	The cost of selling electricity (¥)
C_{gas}	The gas cost (¥)
C_{mai}	Equipment maintenance and investment cost (¥)
C_{Tot}	Comprehensive cost (¥)
COP_{HP}	Heating coefficient of heat pump
COP_{LBR}	Refrigeration coefficient
COP_{qe}	The refrigeration factor of the electric refrigerator
$E_{e,in}$	The electric energy of the power (kW)
ER	Electric refrigerator
$F_{GT,in}$	Natural gas input for the gas turbine (kJ)
$F_{n,GT}$	The gas turbine rate offset function (kJ)
GB	Graphene battery
GT	Gas turbine
HE	Heat exchanger
HP	Heat pump
HS	Molten salt heat storage tank
I_{IN}	The actual light intensity (A)
I_{TE}	The actual sunlight intensity (A)
LBR	Lithium bromide refrigerator with flue gas and hot water
η_{HP}	Heating recovery efficiency of heat pump
η_{HE}	Heat exchange efficiency of heat exchanger
np	The percentage corresponding to the gas turbine gear
η_{GT}	The electricity generation efficiency of the gas turbine
η_{LBR}	Recovery efficiency of lithium bromide refrigerator with flue gas and hot water
η_{qe}	Refrigeration efficiency of the electric refrigerator
η_{HS}^{CH}	The efficiency of heating storage of the molten salt heat storage tank
η_{HS}^{DI}	The efficiency of heating release of the molten salt heat storage tank
η_{WST}^{CH}	The efficiency of cooling of water storage tank
η_{WST}^{DI}	The efficiency of cooling release of water storage and storage tank
η_{GB}	The self-discharge efficiency of graphene cells
η_{GB}^{CH}	Charging efficiency of graphene batteries

η_{GB}^{DI}	Discharging efficiency of graphene batteries
η_{WP}	The electric energy conversion efficiency
PG	Photovoltaic generator
P_{GT}	The output of gas turbine (kW)
P_{GT}^*	Standard value of the generating electricity of the gas turbine (kW)
P_{BO}	The rated power of heat boiler (kW)
P_{HP}	The rated power of heat pump (kW)
P_{HE}	The rated power of heat exchanger (kW)
P_{WST}	The rated power of storage tank (kW)
P_{ER}	The rated power of electric refrigerator (kW)
P_{LBR}	The rated power of lithium bromide refrigerator with flue gas and hot water (kW)
P_{GB}	The rated power of graphene battery (kW)
P_{HS}^{CH}	The power of heating storage of the molten salt heat storage tank (kW)
P_{HS}^{DI}	The heating release of the molten salt heat storage tank (kW)
P_{WST}^{CH}	The power of cooling of water storage tank (kW)
P_{WST}^{DI}	The power of cooling release of water storage tank (kW)
P_{GB}^{CH}	The charging electricity of graphene batteries (kW)
P_{GB}^{DI}	The discharging electricity of graphene batteries (kW)
P_{PG}	The electricity generation electricity (kW)
P_{TE}	Maximum test electricity of photovoltaic generator (kW)
P_{WG}	The output electric power of the wind turbine (kW)
$p_{pow}(t)$	Electricity price at time t (¥)
$C_{pow}(t)$	Electricity purchase at time t (¥)
Q_{BO}	The recovered heating of the heat boiler (kJ)
$Q_{BO,in}$	The recovered input heating of the heat boiler (kJ)
Q_{HE}	Output heating of the heat exchanger (kJ)
$Q_{HE,in}$	Input heating of the heat exchanger (kJ)
Q_{HP}	Heating capacity of heat pump (kJ)
Q_{HP}^*	Flue gas heating recovery of the heat pump (kJ)
$Q_{HP,in}$	Input heating of heat pump (kJ)
Q_{LBR}	Output heating of lithium bromide refrigerator (kJ)
$Q_{LBR,in}$	Input heating of lithium bromide refrigerator (kJ)
Q_{LBR}^*	Heat recovery from lithium bromide refrigerator (kJ)
S_{HS}^t	Heating reserve state of a molten salt heat storage tank at t moment (kJ)
S_{WST}^t	The cooling load storage state of the water storage tank at t moment (kJ)
S_{GB}^t	The electric load reserve state of graphene battery at t moment (kJ)

T_{OP}	The operating temperature of the photovoltaic cells ($^{\circ}\text{C}$)
T_{EN}	The ambient temperature of the photovoltaic cells ($^{\circ}\text{C}$)
$v_{GT, gas}(t)$	The actual inlet rate of the gas turbine during the full load operation (kg/min)
$v_{HP, gas}(t)$	The actual inlet rate during the heat pump operation (kg/min)
$v_{BO, gas}(t)$	The actual inlet rate of the heat boiler during full-load operation (kg/min)
$v_{HE, gas}(t)$	The actual gas inlet rate of heat exchanger (kg/min)
$v_{HE, wat}(t)$	The water inlet speed of heat exchanger (t/min)
$v_{LBR, gas}(t)$	The actual gas inlet velocity of the lithium bromide refrigerator (kg/min)
$v_{RE, wat}(t)$	Water inlet velocity of the lithium bromide refrigerator (t/min)
WG	Wind generator
WST	Water storage tank

production process of titanium dioxide. The author uses the CCHP system to provide energy for the production process of titanium dioxide at different temperatures. However, the author only takes the CCHP system as a separate energy supply system. As a result, this method cannot solve the problem of chemical waste heat emission and economic cost, and cannot be applied in practice.

Nowadays, the CCHP system still has various deficiencies. Firstly, because most of the heating recovery equipment of CCHP systems is the heat boiler, the waste heating source can only be exhaust gas, and another format of waste heat (wastewater heating) is difficult to recover. Moreover, the heating recovery capacity of the system needs to be improved so that the system's limitation is enhanced. Jiazheng et al. (2022) and others study the air-source heat pump water heater and analyze that its heating COP is greater than that of the compression system. Mingzhe et al. (2022) and others design an office building for the sewage-source heat pump system of the sewage treatment plant, recycling sewage for regeneration and heating feedback. Lu et al. (2022) and Ai et al. (2022) study the energy cascade heating recovery to improve system efficiency. According to the above scholars' analysis, the heat efficiency of heat pump in recycling waste water is very obvious. But the application of heat pump in chemical waste heat recovery has not been realized.

Secondly, CCHP system energy storage mainly includes electricity storage, heating storage and cooling storage. As a new type of battery, graphene battery completes the charging and discharging function by rapidly shuttling lithium ions between graphene surface and electrode. Yuanyuan et al. (2022) and others tested the graphene battery and showed excellent cycle and rate performance. Graphene battery is suitable for high-power charging and discharging places. Guanghua (2019) simulated a variety of heat storage equipment. Molten salt heat storage tank can be outstanding in both economic and environmental aspects. Its thermal storage performance is also excellent. Leitian and Hang (2018) and others applied water storage tank to automobile industrial park. Scholars selected 92 800 kW water storage tank, which can ensure the stable supply of 10–16 $^{\circ}\text{C}$ chilled water. The results show that the water storage tank has good cooling storage efficiency and economic benefits. However, the above energy storage equipment has hardly been applied to the CCHP system.

Thirdly, the energy supply system contains three kinds of energy flows: cooling, heating, and electricity, and the construction of the CCHP system are complex. Therefore, the control strategy of the complex system is also a problem for the optimal energy output. Li et al. (2022) and others, combining multiple CCHP systems, manage the energy coordination between various approaches to achieve the purpose of energy complementarity between systems. Based on the time-of-use electricity price strategy, Cui et al. (2022) and others establish the variable load model according to the user's room temperature comfort requirements and the allowable fluctuation range of domestic hot water temperature to realize the control of system load. Zhang et al. (2022) and others implement a master-slave operation strategy based on integrated energy system operators, enterprises move, set up operation framework to achieve system operation. Cheng et al. (2022) and others obtain the optimal power allocation scheme of the system equipment by combining day-ahead scheduling with a day-ahead scheduling strategy. Jianmin et al. (2022) and others propose the hybrid load following a strategy of energy storage characteristics to realize the storage and release of system energy and reduce energy waste. The above scholars have proposed various CCHP systems, but most of them cannot adapt to chemical enterprises. It is particularly important to consider a CCHP system that can be combined with chemical process.

Finally, because it is a complex multi-functional system, resulting high cost of energy supply, many enterprises still choose to purchase electricity directly to fulfill cooling, heating, and electricity demands. This increases the cost of additional equipment for the enterprise itself and poses a challenge to grid stability. The combined cost is too high, indicating that the system's internal energy load scheduling is improper and the energy efficiency is not optimal. Optimization algorithms are better solutions to optimize the complex energy system's operation. By applying the algorithms to the control strategy, optimal scheduling of system load can be realized. Such as Liang et al. (2021) and others use the decomposition-based multi-objective optimization algorithm for economic, energy consumption, and emissions three aspects to establish models and solve the optimal scheduling scheme. Tooryan et al. (2022) and others use a heuristic particle swarm optimization algorithm to find the optimal energy management scheme so that the system's natural gas consumption is reduced by 6.2%, and emissions are also significantly reduced. Keskin and Soykan (2022) and others use mixed integer linear programming (MILP), a mathematical solution that reduces the cost of the system by 40.3%, with an investment return expected to be 6.6 years. Liang et al. (2022) and others use the feature line method to alternate the two-layer model to obtain an accurate scheduling scheme. Guian et al. (2022) and others use the improved dynamic inertia weight particle swarm algorithm to solve the cost of each system and verify the effectiveness of the optimal economic cooling, heating, and power model. The above scholars all use various optimization scheduling methods to optimize the CCHP system, but they cannot reflect the optimization of the recovery benefits of chemical waste heat.

Although many scholars have made in-depth research on CCHP, there are still many shortcomings to be remedied. The CCHP system that can simultaneously realize the chemical wastewater recovery and economic optimal scheduling has not yet appeared.

Inspired by the research of the above scholars, in this paper, the multi-stage recycling of chemical waste heat, coupling wind and solar power generation equipment and energy storage equipment are deeply studied and analyzed. And the improved algorithm and equipment grading adjustment are used to optimize the scheduling to obtain the optimal economic cost. The research idea of this paper is conceived, as shown in Fig. 1.1:

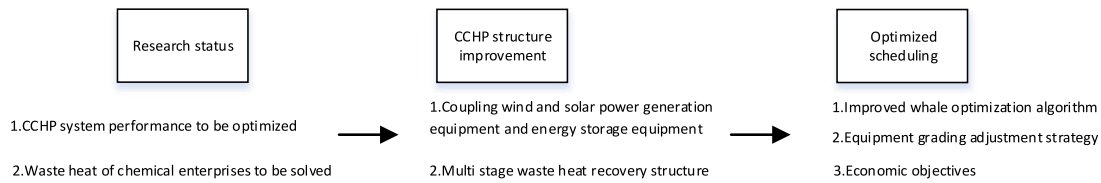


Fig. 1.1. Overall research roadmap.

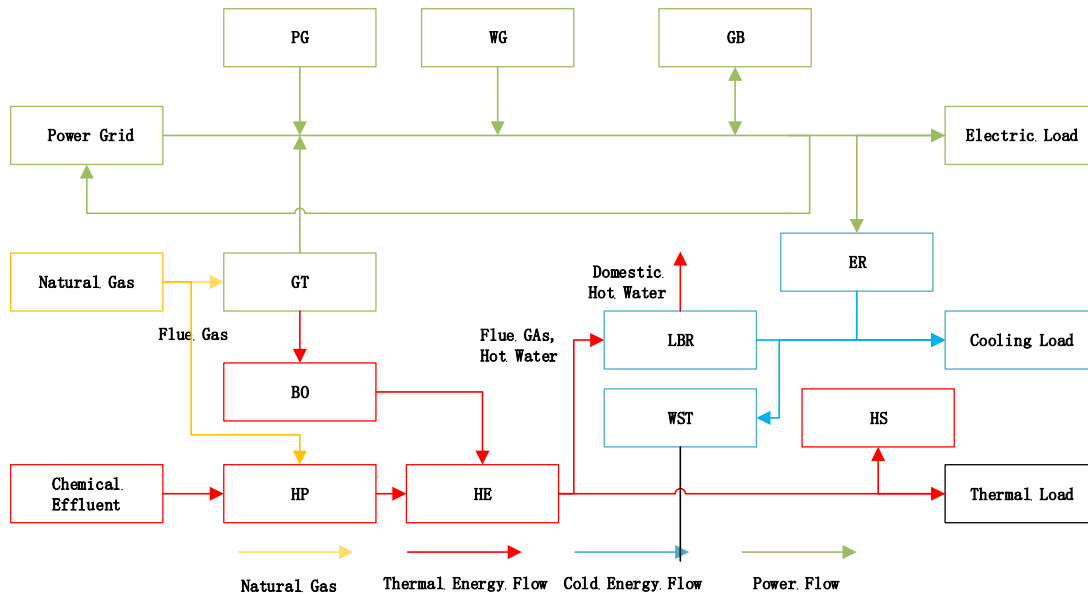


Fig. 2.1. Framework of CCHP system absorbing chemical waste heating.

According to the research in the above literature, this paper intends to use the whale optimization algorithm to improve a new structure CCHP system's operation. This paper presents the optimization solution of the system's operation with optimal cost management through an improved whale optimization algorithm. The reliability and accuracy of the accepted model are verified by simulation and comparative experiments. A chemical enterprise in Jiangsu Province is selected as a case study to analyze the optimization and cost management of the new CCHP structure system.

2. Methodology of CCHP system

In order to solve the waste heat problem of chemical enterprises, the CCHP system is different from the traditional CCHP system and needs further structural adjustment and optimization. Therefore, in this paper, a new type of CCHP system is designed, and an optimization and cost management study is carried out on the new structure CCHP system.

2.1. Framework of the new structure CCHP system

Firstly, in order to recycle chemical waste heat and integrate green energy and energy storage equipment. A new type of CCHP is proposed.

The CCHP system proposed in this paper absorbs the waste heat of the chemical industry. It adapts to chemical enterprises through the structure of the heat pump to recover chemical wastewater to realize the recovery and utilization of waste heat sources in the chemical process by the combined cooling, heating, and electricity generation system. The system includes four parts: the electricity part, heating part, cooling part, and energy storage units. The system frame diagram is shown in Fig. 2.1:

The electricity includes a gas turbine, photovoltaic generator, wind turbine, graphene battery, and power grid. The main electricity generation equipment is a gas turbine with natural gas as a fuel supply. Photovoltaic generators, wind turbines, and graphene batteries are auxiliary electricity supply equipment. The system is incorporated into the power grid. Under insufficient or redundant electricity supply, power is purchased and sold to realize the interaction between electricity storage, equipment supply, and electricity dispatching.

The heating part includes a heat pump, heat boiler, heat exchanger, and molten salt heat storage tank. The high-temperature flue gas discharged by a gas turbine is recovered by a heat boiler and converted into hot water for output. The heat pump is used to retrieve the low-temperature wastewater discharged from the chemical process. The waste heating in the wastewater is recycled and converted into high heating. The wastewater and heating of the heat exchanger are transferred to the untreated flue gas in the boiler, and the residual heating of the heat exchanger is further recovered. The function of the molten salt heat storage tank is to supplement or store heating.

The cooling part mainly includes lithium bromide refrigerators with flue gas, electric refrigerators, and water storage tanks. The hot water and gas remaining in the heat exchanger are used as the driving heating sources of the lithium bromide refrigerator with flue gas, and the cooling capacity is obtained for output. When the cooling capacity of the hot-water lithium bromide refrigerator is insufficient, the electric refrigerator runs and supplies the cooling. The function of the water storage tank is to supplement or store the cooling capacity in the system.

The energy storage part mainly includes a graphene battery, water storage tank, and molten salt heat storage tank. Three energy storage devices charge and discharge energy for electricity,

cooling, and heating. When the specific system load is redundant or insufficient, they start to operate to make full use of energy.

2.2. Mathematical model of new CCHP system

According to the new CCHP structure proposed above, mathematical modeling is carried out for each equipment. In this way, the theoretical model can be mathematically used for subsequent simulation.

2.2.1. Model of gas turbine

The gas turbine is the main power generation equipment of CCHP, and its electricity generation efficiency is greatly affected by the motor's output. The third-order model can better realize the output fluctuation of the gas turbine.

$$\begin{cases} P_{GT} = \eta_{GT} F_{GT,in} \\ \eta_{GT} = (a_1 + a_2 P_{GT}^{*2} + a_3 P_{GT}^{*3}) / 100 \end{cases} \quad (1)$$

where P_{GT} is the gas turbine output electric power, $F_{GT,in}$ is natural gas input for the gas turbine, η_{GT} is the electricity generation efficiency of the gas turbine, a_1, a_2, a_3 are the electricity generation coefficient of this gas turbine is constant, P_{GT}^* is the standard value of the generating electricity of the gas turbine.

For the step-by-step adjustment of the gas turbine, the speed control of the gas turbine inlet is realized by adjusting the motor speed of the equipment. Among them, the gear adjustment has a certain influence on the motor speed fluctuation. When the gear is low, the speed control of the motor fluctuates wildly, and the speed increase is relatively slow. The classification adjustment rate is supplemented by introducing the performance offset function. For the convenience of calculation, the motor's full load is regarded as a non-performance deviation. The rate control is as follows:

$$v_{GT,gas}(t) = \begin{cases} a_{GT,1} * t^{m_1} + F_{n,GT} & t < t_0 \\ np * v_{GT,max} & t \geq t_0 \end{cases} \quad (2)$$

$$F_{n,GT} = (v_1 + v_2 + \dots + v_n) / n \quad (3)$$

where $a_{GT,1}$ is the gas inlet rate coefficient of the gas turbine in operation, t is the equipment running time, t_0 is the time required for the gas inlet rate to increase to the peak value, $v_{GT,max}$ is maximum gas inlet rate during the full load operation, $v_{GT,gas}(t)$ is the actual inlet rate of the gas turbine during the full load operation, m_1 is the constant, 100% gear set 1.75% gear set 0.8,50% gear set 0.6,25% gear setting 0.4, np is the percentage corresponding to the gas turbine gear, according to the different gears is set at 100%, 75%, 50%, and 25%, $F_{n,GT}$ is the gas turbine rate offset function, v_1, v_2, \dots, v_n are the inlet rate sampled for the upper cycle, n is the sample coefficients sampled for the last period.

2.2.2. Model of heat boiler

As a heat boiler of flue gas recovery equipment and preliminary heating recovery equipment, the linear change of heating of the heat boiler is indicated by the waste heating recovery efficiency (η_{BO}) of the equipment itself.

$$Q_{BO} = \eta_{BO} Q_{BO,in} \quad (4)$$

where $Q_{BO}, Q_{BO,in}$, respectively, are the recovered heating and input heating of the heat boiler, η_{BO} is the waste heating recovery efficiency of the heat boiler.

For the heat boiler, the gear speed control of the flue gas recovery module's motor makes the gear of gas inlet speed adjustment of the heat boiler.

$$v_{BO,gas}(t) = \begin{cases} a_{BO,1} * t^{m_2} & t < t_1 \\ n * v_{BO,max} & t \geq t_1 \end{cases} \quad (5)$$

where $a_{BO,1}$ is the gas inlet rate coefficient of the heat boiler in operation, t is running time, t_1 is the time required for the inlet rate to increase to the peak, m_2 is the constant, 100% gear set 1.75% gear set 0.8,50% gear set 0.6,25% gear setting 0.4, $v_{BO,max}$ is the maximum flue gas inlet rate of the heat boiler in operation, $v_{BO,gas}(t)$ is the actual flue gas inlet rate of the heat boiler during full-load operation.

2.2.3. Model of heat pump

The heat pump is the main equipment for the recovery of chemical wastewater. Its heating recovery efficiency (η_{HP}) and heating coefficient (COP_{HP}) represent the change of input and output of the equipment. And η_{HP} represents the output fluctuation of the heat pump through the third-order model.

$$\begin{cases} Q_{HP} = \eta_{HP} COP_{HP} Q_{HP,in} \\ \eta_{HP} = (b_1 + \frac{b_2}{Q_{HP}^{*2}} + \frac{b_3}{Q_{HP}^{*3}}) \end{cases} \quad (6)$$

where $Q_{HP}, Q_{HP,in}$ are heating capacity and input heating of heat pump, η_{HP} is the heating recovery efficiency of the heat pump, COP_{HP} is the heat coefficient of the heat pump, b_1, b_2, b_3 are heating constants of the heat pump, Q_{HP}^* is flue gas heating recovery of the heat pump.

For the heat pump for gear adjustment, through the heat pump input module, to control the motor speed of the chemical wastewater pump, to realize the control of the heat pump water inlet rate.

$$v_{HP,wat}(t) = \begin{cases} a_{HP,1} * t^{m_3} & t < t_2 \\ n * v_{HP,max} & t \geq t_2 \end{cases} \quad (7)$$

where $a_{HP,1}$ is the water inlet speed coefficient of the heat pump operation, t is running time, t_2 is the required time for the water inlet velocity to increase to the peak point, m_3 is the constant, 100% gear set 1.75% gear set 0.8,50% gear set 0.6,25% gear setting 0.4, $v_{HP,max}$ is the maximum water inlet rate when the heat pump runs at full load, $v_{HP,gas}(t)$ is the actual water inlet rate during the heat pump operation.

2.2.4. Model of heat exchanger

The heat exchanger is the main equipment for the system to recover the heating of flue gas and hot water. The heat exchange efficiency (η_{HE}) of the heat exchanger expresses the linear relationship between the heating input and output.

$$Q_{HE} = \eta_{HE} Q_{HE,in} \quad (8)$$

where $Q_{HE}, Q_{HE,in}$ are the output heating and the input heating of the heat exchanger, respectively, η_{HE} is the heating exchange efficiency of the heat exchanger.

For the control of the heat exchanger, the pumping motor and the gas recovery motor should be rate-controlled separately to realize the gear adjustment of the heat exchanger.

$$v_{HE,gas}(t) = \begin{cases} a_{HE,1} * t^{m_4} & t < t_3 \\ n * v_{HE,max1} & t \geq t_3 \end{cases} \quad (9)$$

$$v_{HE,wat}(t) = \begin{cases} a_{HE,2} * t^{m_4} & t < t_4 \\ n * v_{HE,max2} & t \geq t_4 \end{cases} \quad (10)$$

where $a_{HE,1}, a_{HE,2}$ are the gas and water inlet rate coefficient of the heat exchanger during operation, t is running time, t_3, t_4 are the required time for the gas and water inlet rate to increase to the peak, m_4 is the constant, 100% gear set 1.75% gear set 0.8,50% gear set 0.6,25% gear setting 0.4, $v_{HE,max1}, v_{HE,max2}$ are the maximum gas and water inlet rate when the heat exchanger is fully loaded, $v_{HE,gas}(t), v_{HE,wat}(t)$ are the actual gas and the water inlet rate when the heat exchanger runs.

2.2.5. Model of lithium bromide refrigerator with flue gas and hot water

The heat exchanger is the leading equipment for further recovering heating from flue gas and hot water. It is driven by the flue gas and hot water as heating sources. The refrigeration coefficient (COP_{LBR}) and the recovery efficiency (η_{LBR}) of the flue gas and hot water indicate the relationship between the input heating quantity and the output cooling volume of the equipment. A third-order model represents the recovery efficiency (η_{LBR}). This represents the fluctuation of equipment cooling capacity.

$$\begin{cases} Q_{LBR} = \eta_{LBR} COP_{LBR} Q_{LBR,in} \\ \eta_{LBR} = (c_1 + \frac{c_2}{Q_{LBR}^*} + \frac{c_3}{Q_{LBR}^{*2}}) \end{cases} \quad (11)$$

where respectively, Q_{LBR} , $Q_{LBR,in}$ are output and input heating of lithium bromide refrigerator, COP_{LBR} is refrigeration coefficient of lithium bromide refrigeration, η_{LBR} is the recovery efficiency of the gas and hot water for the lithium bromide refrigerant machine, c_1 , c_2 , c_3 are the refrigeration constant of the lithium bromide refrigerant machine, Q_{LBR}^* is heat recovery from gas and water of lithium bromide refrigerator.

For the control of the lithium bromide refrigerator, the pumping motor and the flue gas recovery motor should be rate-controlled, respectively, to realize the gear adjustment of the equipment.

$$v_{LBR,gas}(t) = \begin{cases} a_{LBR,1} * t^{m_5} & t < t_5 \\ n * v_{LBR,max1} & t \geq t_5 \end{cases} \quad (12)$$

$$v_{LBR,water}(t) = \begin{cases} a_{LBR,2} * t^{m_5} & t < t_6 \\ n * v_{LBR,max2} & t \geq t_6 \end{cases} \quad (13)$$

where $a_{LBR,1}$, $a_{LBR,2}$ are the gas and water inlet coefficient of lithium bromide refrigerator, t is running time, t_5 , t_6 are the required time for the gas and water inlet rate to increase to the peak, m_5 is the constant, 100% gear set 1.75% gear set 0.8, 50% gear set 0.6, 25% gear setting 0.4, $v_{LBR,max1}$, $v_{LBR,max2}$ are maximum gas and water inlet velocity of lithium bromide refrigerator, $v_{LBR,gas}(t)$, $v_{LBR,water}(t)$ are the actual gas and water inlet velocity of the lithium bromide refrigerator.

2.2.6. Model of electric refrigerator

The electric refrigerator makes the cooling amount through electric power, and its expression is:

$$Q_{ER} = E_{e,in} * \eta_{qe} * COP_{qe} \quad (14)$$

where $E_{e,in}$ is to absorb the electric energy of the power grid, η_{qe} is the refrigeration efficiency of the electric refrigerator, COP_{qe} is the refrigeration factor of the electric refrigerator.

2.2.7. Model of molten salt heat storage tank

The molten salt heat storage tank is a system heating storage equipment, and the running states are indicated as follows:

$$S_{HS}^t = S_{HS}^{t-1} + \eta_{HS}^{CH} P_{HS}^{CH} - \eta_{HS}^{DI} P_{HS}^{DI} \quad (15)$$

where respectively, S_{HS}^t , S_{HS}^{t-1} are the heating reserve state of a molten salt heat storage tank at $t - 1$, t moment, η_{HS}^{CH} , η_{HS}^{DI} are the efficiency of heating storage and heating release of the molten salt heat storage tank, respectively, P_{HS}^{CH} , P_{HS}^{DI} are the power of heating storage and heating release of the molten salt heat storage tank, respectively.

2.2.8. Model of water storage tank

The water storage tank is a system of cooling storage equipment, and its running states are as follows:

$$S_{WST}^t = S_{WST}^{t-1} + \eta_{WST}^{CH} P_{WST}^{CH} - \eta_{WST}^{DI} P_{WST}^{DI} \quad (16)$$

where S_{WST}^t , S_{WST}^{t-1} are the cooling storage state of the water storage tank at $t - 1$, t moment, η_{WST}^{CH} , η_{WST}^{DI} are the efficiency of cooling storage and cooling release of water storage tanks, respectively, P_{WST}^{CH} , P_{WST}^{DI} are the power of cooling storage and cooling release of water storage tank respectively.

2.2.9. Model of graphene battery

The graphene battery is electricity storage equipment for the system, and the charge and discharge process is also self-discharge. The process is as follows:

$$S_{GB}^t = (1 - \eta_{GB}) S_{GB}^{t-1} + \eta_{GB}^{CH} P_{GB}^{CH} - \eta_{GB}^{DI} P_{GB}^{DI} \quad (17)$$

where S_{GB}^t , S_{GB}^{t-1} are the electric load reserve state of graphene battery at $t - 1$, t moment, η_{GB} is the self-discharge efficiency of graphene cells, η_{GB}^{CH} , η_{GB}^{DI} are the charging and discharging efficiency of graphene batteries, P_{GB}^{CH} , P_{GB}^{DI} are the charging and discharge electricity of graphene batteries, respectively.

2.2.10. Model of photovoltaic generator

The photovoltaic generator is one of the auxiliary electricity generation equipment of the system. By testing the electricity generation electricity (P_{PG}) and testing the actual light intensity (I_{IN}), the actual photovoltaic electricity generation electricity is calculated. The formula is as follows:

$$P_{PG} = \frac{I_{TE}(1 + K(T_{OP} - T_{EN}))P_{TE}}{I_{IN}} \quad (18)$$

where P_{PG} is the output of the photovoltaic generator set, I_{TE} , I_{IN} are the actual sunlight intensity and the light intensity under the standard test conditions (1 kW/m² light intensity, ambient temperature of 25 °C), respectively, K is the temperature coefficient, P_{TE} is maximum test electricity of photovoltaic generator set under standard test conditions, T_{OP} , T_{EN} are the operating temperature and ambient temperature of the photovoltaic cells, respectively.

2.2.11. Model of wind turbine generator

As one of the auxiliary electricity generation equipment of the system, the wind turbine represents the output of the wind turbine through the air density (ρ), the generator blade radius (R), the speed of the wind blowing (v) from the outside world and the electric energy conversion efficiency (η_{WP}).

$$\begin{cases} P_{WG} = \frac{1}{2} \rho \pi R^2 v^3 \eta_{WP} \\ \eta_{WP} = f(\theta, \lambda) \\ \lambda = \frac{\omega_{WG} R}{v} \end{cases} \quad (19)$$

where P_{WG} is the output electric power of the wind turbine, ρ , R , v , η_{WP} are air density, blade radius of the wind turbine, the speed of the external wind, and the conversion efficiency of wind energy, θ , λ are rate ratio of blade pitch Angle and blade tip, ω_{WG} is the mechanical angular speed of the wind turbine.

3. Optimal scheduling model of CCHP system

On the basis of the equipment modeling of the CCHP system, this paper puts forward an operation strategy of graded regulating equipment, which can realize the internal energy scheduling of the system.

3.1. System load scheduling strategy

In this paper, the appropriate equipment sets are 0%, 25%, 50%, 75%, and 100% to achieve the system energy flow control through the cooling, heating, and electricity supply equipment for gear control. The main idea of specific gear control is to regulate the equipment's input port and the input size to achieve output control.

The specific parameters are the inlet natural gas flow rate of the gas turbine, pumping speed of the heat pump, inlet gas and hot water flow rate of the heat exchanger, and inlet gas and hot water flow rate of lithium bromide refrigerator. Finally, the electric refrigerator is cooled by electricity. This paper uses an electric refrigerator with a frequency conversion function. The inverter controls the compressor speed in the electric refrigerator to control the input cooling capacity.

The corresponding supply equipment sets the output power level adjustment to realize the cooling, heating, and electricity load schedule.

In the cooling energy flow, the output power of the lithium bromide refrigerator and the electric refrigerator is controlled. The cooling load scheduling strategy is that, under normal operation, the lithium bromide refrigerator has a higher priority (priority to obtain cooling capacity through the recovered heating of the system). When the cooling transmitted by the refrigerator is insufficient to meet the needs of chemical enterprises, the electric refrigerator starts and gradually increases the gear according to the demand to fully dispatch the cooling load and ensure the full application of energy in the cooling energy flow. Finally, in winter, the demand of chemical enterprises for cooling load is almost negligible, so when the system runs in winter, the two refrigeration equipment is always at 0% level.

The output power of the heat boiler, heat pump, and heat exchanger is controlled to realize heating dispatching in the heating flow. The strategy is that during normal operation, the heat boiler, heat pump, and heat exchanger are operated at 75% or 100% level in the working period of chemical enterprises, and the user side is continuously heated. During the off-time period of the worker, the heating demand decreases, and the related equipment reduces the gear, using half or low power operation. Finally, in summer, the need for heating of chemical enterprises is reduced. Heat boilers and heat pumps are the recovery equipment of flue gas and wastewater, and they are still running. The heat exchanger can maintain 0% or 25% gear so that the recovered flue gas and hot water can fully replace the cooling capacity.

The electricity flow is mainly through the gas turbine output power to electricity schedule. The output of wind turbines and photovoltaic generators is affected by local wind and light energy and is not controlled. The electricity dispatching strategy is that the gas turbine of chemical enterprises operates at 75% or 100% gear during the normal working period and operates at half load or low load during the night or after work. Finally, when the electricity output exceeds the demand of chemical enterprises, it can be sold to the large grid and fed back to the grid.

There is corresponding energy storage equipment for cooling, heating, and electricity flow, including the water storage tank, molten salt storage tank, and graphene battery. The three roles are storing at low load demand, releasing energy at peak load consumption, and realizing auxiliary scheduling of three loads. The system energy scheduling strategy is shown in Fig. 3.1:

3.2. Optimal scheduling model of CCHP system for absorption of chemical waste heating

In order to achieve the system economic goal, the economic goal model is built on the basis of the above system mathematical model and operation strategy.

3.2.1. Equipment maintenance and investment cost

The combined CCHP system operating equipment for absorbing chemical waste heating includes the gas turbine, heat boiler, heat pump, heat exchanger, lithium bromide refrigerator, electric refrigerator, molten salt heat storage tank, water storage tank, graphene battery, photovoltaic generator, and wind turbine. The above equipment is to ensure the service life, chemical process safety, and the need for equipment purchase and maintenance. The following formula is for the system equipment maintenance and investment cost:

$$C_{mai} = k_{GT}P_{GT} + k_{BO}P_{BO} + k_{HP}P_{HP} + k_{HE}P_{HE} + k_{LBR}P_{LBR} + k_{ER}P_{ER} + k_{HS}P_{HS} + k_{WST}P_{WST} + k_{GB}P_{GB} + k_{PG}P_{PG} + k_{WG}P_{WG} + C_{buy_sys}/y_{use} \quad (20)$$

where P_{GT} , P_{BO} , P_{HP} , P_{HE} , P_{LBR} , P_{ER} , P_{HS} , P_{WST} , P_{GB} , P_{PG} , P_{WG} are the output power of the gas turbine, heat boiler, heat exchanger, lithium bromide refrigerator, electric refrigerator, molten salt heat storage tank, water storage tank, graphene battery, photovoltaic generator and wind turbine, respectively. k_{GT} , k_{BO} , k_{HP} , k_{HE} , k_{LBR} , k_{ER} , k_{HS} , k_{WST} , k_{GB} , k_{PG} , k_{WG} are maintenance cost of unit electric power of the gas turbine, heat boiler, heat exchanger, lithium bromide refrigerator, electric refrigerator, molten salt heat storage tank, water storage tank, graphene battery, photovoltaic generator and wind turbine, respectively. C_{buy_sys} is purchase cost of CCHP unit. y_{use} is unit service life.

3.2.2. Electricity purchasing cost

The CCHP system absorbing chemical waste heating is mainly supplied by the gas turbine, followed by photovoltaic and wind turbines as auxiliary electricity generation. Finally, the graphene battery is charged and discharged. However, due to the great demand for electricity in chemical enterprises, purchasing electricity from the grid is necessary when the above electricity is insufficient. The cost of buying electricity is as follows:

$$C_{pow} = \sum_{t=1}^T p_{pow}(t)G_{pow}(t) \quad (21)$$

where $p_{pow}(t)$ is electricity price at time t , $G_{pow}(t)$ is electricity purchase at time t .

3.2.3. Electricity sales cost

When the CCHP system has a sufficient electricity supply and the storage capacity of graphene batteries have reached a threshold, multiple electricity can be sold back to the grid. The following is the cost formula:

$$C_{sell} = \sum_{t=1}^T p_{sell}(t)G_{sell}(t) \quad (22)$$

where $p_{sell}(t)$ is selling tariff at time t , $G_{sell}(t)$ is electricity sales at time t .

3.2.4. Gas cost

In order to reduce environmental pollution, the supply fuel of this system is natural gas with economic and environmental protection, and its price is relatively fixed.

$$C_{gas} = k_{gas} \sum_{t=1}^T G_{gas}(t) \quad (23)$$

where k_{gas} is natural gas prices, $G_{gas}(t)$ is gas purchase at time t .

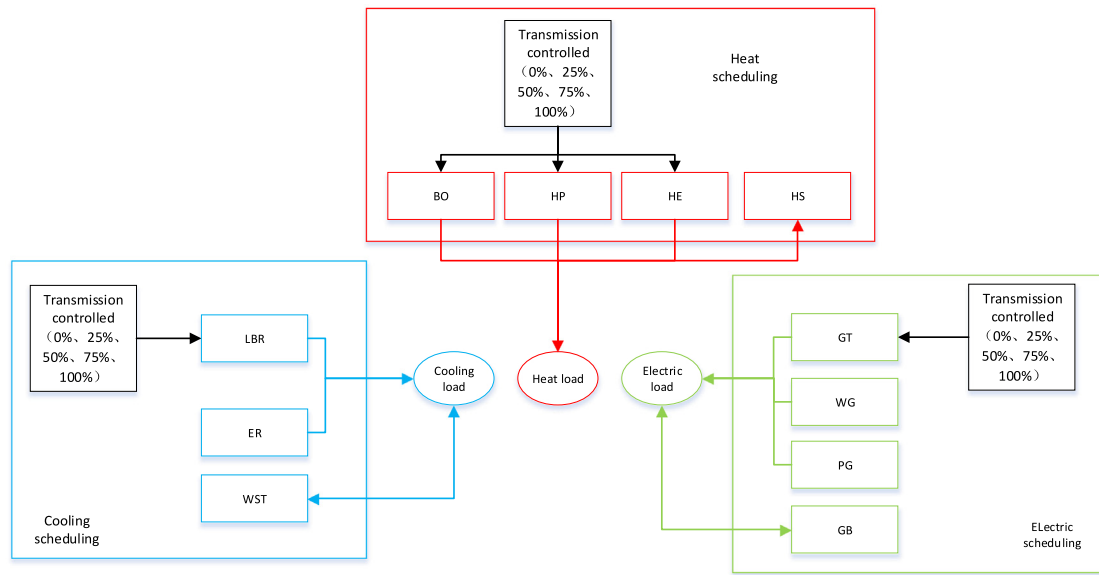


Fig. 3.1. Energy scheduling policy diagram.

3.2.5. Environmental governance cost

Industrial enterprises greatly impact the surrounding environment, so for the long-term development of the factory, it is necessary to treat the discharged sewage or gas (CO₂, SO₂, NO_x).

$$C_{pul} = (1 - \eta_{air}) \left(\sum_{t=1}^T p_{car} G_{car}(t) + \sum_{t=1}^T p_{SO_2} G_{SO_2}(t) + \sum_{t=1}^T p_{NO_x} G_{NO_x}(t) \right) + \eta_{wat} \sum_{t=1}^T p_{wat} G_{wat}(t) \quad (24)$$

where $G_{car}(t)$ is CO₂ emissions per 1 kWh equipment consumption at time t , p_{car} is treatment cost per 1 kg CO₂, $G_{SO_2}(t)$ is SO₂ emissions per 1 kWh equipment consumption at time t , p_{SO_2} is treatment cost per 1 kg SO₂, $G_{NO_x}(t)$ is NO₂ emissions per 1 kWh equipment consumption at time t , p_{NO_x} is treatment cost per 1 kg NO₂, $G_{wat}(t)$ is emissions of chemical wastewater per 1 kWh equipment consumption at time t , p_{wat} is treatment cost per 1 t chemical wastewater, η_{air} is system gas recovery efficiency, η_{wat} is wastewater recovery efficiency of the system.

3.2.6. Objective function

This paper takes the comprehensive cost as the optimization goal of the system, mainly including equipment maintenance and investment cost, electricity purchase cost, electricity sales cost, natural gas cost, and environmental governance cost. The objective function of the system is as follows:

$$\min C_{Tot} = \min(C_{mai} + C_{pow} + C_{gas} + C_{pul} - C_{sell}) \quad (25)$$

where C_{Tot} is the comprehensive cost of the CCHP system, C_{mai} is equipment maintenance and investment cost, C_{pow} is electricity purchasing cost, C_{sell} is electricity sales cost, C_{gas} is gas cost, C_{pul} is environmental governance cost.

3.2.7. Cooling, heating, and electricity balance constraints

According to the first law of thermodynamics, the cooling, heating, and electricity of the CCHP system must be input and output balanced to meet the actual situation. The formula is as follows:

$$Q_{BO} + Q_{HP} + Q_{HE} + Q_{HS} = Q_{heat} \quad (26)$$

$$Q_{LBR} + Q_{ER} + Q_{WST} = Q_{cold} \quad (27)$$

$$P_{GT} + P_{PG} + P_{WG} + P_{GB} + P_{grid} - P_{ERP} = P_{power} \quad (28)$$

where Q_{BO} is heating generated by heat boiler; Q_{HP} is heating generated by the heat pump; Q_{HE} is heating generated by heat exchanger; Q_{HS} is heating generated by molten salt heat storage tank; Q_{heat} is total heating of the system;

Q_{LBR} is the cooling generated by lithium bromide refrigerator; Q_{ER} is cooling generated by the electric refrigerator; Q_{WST} is the cooling generated by water storage tank; Q_{cold} is total cooling of system.

P_{GT} is electricity from gas turbines; P_{PG} is electricity from photovoltaic generators; P_{WG} is electricity from wind generators; P_{GB} is electricity from graphene battery; P_{ER} is the absorption capacity of the electric refrigerator; P_{grid} is electricity provided by the grid; P_{power} is total electricity of the system;

3.2.8. Load operation condition constraint

Each piece of equipment in the CCHP system has upper and lower power limits. The parameters are determined by the equipment's rated capacity and other related parameters. In order to make the load operation conform to the law, the upper and lower limits of related equipment are set, and the constraint formula of each system equipment is as follows:

$$P_{GT, min} \leq P_{GT}(t) \leq P_{GT, max} \quad (29)$$

$$P_{BO, min} \leq P_{BO}(t) \leq P_{BO, max} \quad (30)$$

$$P_{HP, min} \leq P_{HP}(t) \leq P_{HP, max} \quad (31)$$

$$P_{HE, min} \leq P_{HE}(t) \leq P_{HE, max} \quad (32)$$

$$P_{LBR, min} \leq P_{LBR}(t) \leq P_{LBR, max} \quad (33)$$

$$P_{ER, min} \leq P_{ER}(t) \leq P_{ER, max} \quad (34)$$

$$P_{PG, min} \leq P_{PG}(t) \leq P_{PG, max} \quad (35)$$

$$P_{WG, min} \leq P_{WG}(t) \leq P_{WG, max} \quad (36)$$

where $P_{GT}(t)$, $P_{BO}(t)$, $P_{HP}(t)$, $P_{LBR}(t)$, $P_{ER}(t)$, $P_{GT}(t)$, $P_{WG}(t)$ are the operation power of the gas turbine, heat boiler, heat pump, heat exchanger, lithium bromide refrigerator, electric refrigerator, photovoltaic generator set, and wind turbine at time t , respectively. $P_{GT, min}$, $P_{BO, min}$, $P_{HP, min}$, $P_{HE, min}$, $P_{LBR, min}$, $P_{ER, min}$, $P_{PG, min}$, $P_{WG, min}$ are minimum output power of corresponding

Table 3.1
Validation of CCHP system for absorption of chemical waste heating.

Key equipment	Model in this paper (MW)	Reference model 1 Yang et al. (2022) (Mw)	Error (%)	Model in this paper (kW)	Reference model 2 Zhuohan et al. (2021) (kW)	Error (%)
GT	600	2.968	0.244	193.938	189.44	0.238
PG	/	/	/	85.001	85.192	0.095
WG	/	/	/	195.728	192.703	0.157
HP	2.162	2.109	0.252	/	/	0.139
BO	0.519	0.511	0.147	/	/	0.265
HE	/	/	/	512.203	494.5	0.358
RE	6.713	6.491	0.342	/	/	0.178
ER	11.187	11.023	0.149	468.534	465	0.076
WST	5.353	5.192	0.311	/	/	0.451
HS	0.467	0.458	0.198	/	/	0.359
BA	1.002	0.982	0.204	851.91	831.62	0.244

equipment. $P_{GT, max}$, $P_{BO, max}$, $P_{HP, max}$, $P_{HE, max}$, $P_{LBR, max}$, $P_{ER, max}$, $P_{PG, max}$, $P_{WG, max}$ are maximum output power of corresponding equipment.

$$S_{HS, min} \leq S_{HS}(t) \leq S_{HS, max} \tag{37}$$

$$S_{WST, min} \leq S_{WST}(t) \leq S_{WST, max} \tag{38}$$

$$S_{GB, min} \leq S_{GB}(t) \leq S_{GB, max} \tag{39}$$

where $S_{HS}(t)$, $S_{WST}(t)$, $S_{GB}(t)$ are heating, cooling, and electricity storage state of the molten salt storage tank, water storage tank, and graphene battery at time t . $S_{HS, min}$, $S_{WST, min}$, $S_{GB, min}$ are the minimum reserve of energy. $S_{HS, max}$, $S_{WST, max}$, $S_{GB, max}$ are the maximum reserve of energy.

In this paper, the mathematical model of the CCHP system with chemical waste heating absorption is established by MATLAB, and a similar structural model by other researchers is based. Combined with the reference model parameters and the results of the working condition diagram, the preliminary simulation comparison and analysis are carried out. The results are shown in Table 3.1:

By comparison, the system output simulation under each working condition shows that the equipment power error is less than 0.5%, and the accuracy is high. Therefore, the scheduling research and optimization research based on this model has practical significance and guiding significance for the system's comprehensive evaluation and subsequent design improvement.

4. Improved whale optimization algorithm

4.1. Whale optimization algorithm

On the basis of the above, the improved whale optimization algorithm is used to realize the energy optimal scheduling of the entire CCHP system, so as to obtain the final optimization result.

Mirjalili and Lewis (2016) and others constructed the whale optimization algorithm through the whale foraging behavior and mathematical modeling. This model simulates three mathematical models: humpback whale foraging, spiral bubble foraging, and random hunting (L, 2021).

(1) Subduction encircles prey

Each whale is equal to an individual in the optimization algorithm and the optimization method of diving around the prey with a probability of 0.5. The individual first surround the prey, and the unique position update formula is as follows:

$$x(T + 1) = x_{best}^*(T) - A * |C * x_{best} - x(T)| \tag{40}$$

$$A = 2a * rand_1 - a \tag{41}$$

$$C = 2 * rand_2 \tag{42}$$

where A and C are vector constant;

$rand_1, rand_2$ are random numbers in [0,1];

x_{best} is current optimal individual location;

$x(T)$ is the individual position of the last iteration;

$x(T + 1)$ is individual location after optimization.

(2) Spiral bubbles

When $|A| < 1$, each whale shrinks and surrounds, with the spiral motion to the prey (optimal individual), the mathematical model is as follows:

$$x(T + 1) = |x_{best} - x(T)| * e^{b * l} \cos(2\pi l) + x_{best} \tag{43}$$

where b is constant;

l is random number in [0,1].

(3) Random search

When $|A| \geq 1$, it represents the outer side of the reshinking range of whale individuals. This part of individuals uses random search to expand the search range and improve the algorithm's accuracy. The mathematical model is as follows:

$$x(T + 1) = x_{rand} - A * |C * x_{best} - x(T)| \tag{44}$$

where x_{rand} is random whale individual location.

However, the basic whale optimization algorithm still has many shortcomings, and the optimization effect for large amounts of data is poor. The main reason is that the mathematical model of the algorithm is that the two main foraging methods of subduction encirclement foraging and spiral bubble foraging are local search optimization methods. Only by randomly searching for prey can the global search be carried out, which is easy to make the optimization results fall into local optimum, resulting in poor accuracy of the optimization results.

As the optimization of the CCHP system in chemical enterprises, this paper takes the comprehensive cost as the optimization variable to minimize the annual output cost. And the system input parameters are more, and the basic whale optimization algorithm cannot meet the system optimization standards.

4.2. Improved whale optimization algorithm

The above description of the basic whale optimization algorithm and the actual requirements of chemical enterprises are necessary to improve the basic whale optimization algorithm. The main purpose is to improve the accuracy of the whale optimization algorithm to achieve the goal of optimal comprehensive cost.

4.2.1. Chaotic strategy (Logistic)

In order to ensure the uniformity and diversity of the initial population of the whale optimization algorithm, logistic mapping (Ahmmmed et al., 2021) is used. The number of initialized populations is N. Logistic chaotic mapping generates chaotic sequences,

which are defined as follows:

$$x_{k+1} = \mu x_k(1 - x_k) \tag{45}$$

where $x_0 \notin \{0, 0.25, 0.5, 0.75, 1.0\}$, $\mu \in [0, 4]$;

x_k is individual last iteration;

x_{k+1} is iterative new generated individual.

After chaotic mapping, initialize the whale population of N d-dimension individuals and randomly produce the first individual. $N-1$ individuals are generated iteratively using the above mapping formula. Finally, the variable value generated by the chaotic mapping is mapped to the whale individual, and the formula is as follows:

$$X = X_{min} + \frac{X_{k+1}}{2} * (X_{max} - X_{min}) \tag{46}$$

where X is individuals after mapping;

X_{min} , X_{max} are lower and upper limits for each individual dimension.

4.2.2. Nonlinearization strategy of convergence factor

In the optimization process of the whale optimization algorithm, the convergence factor a (Meijin, 2021) is a critical parameter. The parameter size replaces the global search and local search. The basic whale optimization algorithm mainly linearly changes the convergence factor from the limited upper limit to the lower limit. This method cannot reflect the actual optimization search process, significantly reducing searchability and accuracy.

Therefore, the convergence factor is nonlinearized in this paper. The nonlinear variation relationship between the convergence factor and the number of iterations is realized through the inverse tangent function's variation law. To improve the probability of global search and local search change, improve the accuracy of the optimization process. The nonlinear variation formula of convergence factor (a) is as follows.

$$a = 5 - 5 * \arctan((T / Max_iter)^{0.6}) \tag{47}$$

where T is the current iteration time;

Max_iter is the maximum number of iterations set by the algorithm.

4.2.3. Nonlinear change strategy of weight factor

In the basic whale optimization algorithm, the weight factor is not introduced in the formula of the optimization process. As a result, the global search ability of the optimization process is poor, and the results easily fall into local optimum. An appropriate weight coefficient will improve the algorithm's global and local search ability (Hui et al., 2021). In order to adjust the ability of global search and local search, the weight factor ω is introduced. When the weight factor is weighted in the optimization process formula, the nonlinear change of the weight factor further improves the ability of global search to improve the algorithm's accuracy. Weight factor expression is as follows:

$$\omega(t) = k * (e^{-\left(\frac{5t}{Max_iter}\right)^{1.5}} + m) \tag{48}$$

where k , m are constant coefficients.

4.2.4. Principle of improved whale optimization algorithm

Through the above three improvements, the structural and content adjustment of the basic whale optimization algorithm is realized, and the goal is to improve the solution accuracy of the algorithm.

Firstly, the improved whale optimization algorithm will initialize the data, eliminate the influence of previous algorithm operations, and input the optimization scheduling model of the

CCHP system that absorbs chemical waste heating into the algorithm. Next, the chaotic logistic strategy makes the algorithm generate uniform and diverse initial populations. Second, enter the main cycle of the whale optimization algorithm. The optimization method is selected by probability p , and the global search and local search are replaced by coefficient constant $|A|$. Finally, calculate the optimal individual through the fitness comparison, and update the value of the optimal individual until the end of the iteration. Fig. 4.2.3 is the flow chart of the improved whale optimization algorithm:

5. System simulation results and analysis

5.1. Load demand and energy scheduling strategy

In this paper, the system is designed to obtain the grading adjustment scheme of each piece of equipment by analyzing the demand load of the CCHP system.

The demand load data come from the comprehensive energy consumption statistics of the local salt production plants published by the local government of Jiangsu and the experimental data itself. The typical demand is selected for use. In this paper, based on the data of two groups of typical days in winter and summer, the design scheme of grading adjustment among the equipment of the CCHP system that absorbs chemical waste heating is obtained.

MATLAB software is used to simulate the CCHP system. Based on the above load scheduling strategy. The gas turbine inlet velocity, inlet velocity of heat boiler, inlet velocity of the heat pump, inlet velocity of the heat exchanger, inlet velocity of lithium bromide refrigerator, and inlet velocity of the internal combustion engine are controlled. The load scheduling of the system improves the overall energy utilization rate so that the supply of cooling, heating, and electricity meets the demand in each time and reduces waste. Combined with the actual load demand of the salt plant, the rate adjustment of equipment import end on typical winter days and typical summer days is shown in Figs. 5.1 and 5.2:

As shown in Fig. 5.1, according to statistics, the typical daily cooling load demand in winter is 198–696 kW, the heating demand is 355–821 kW, and the electricity demand is 356–795 kW. The inlet rate adjustment scheme of equipment under this requirement is obtained through simulation, and the gas inlet rate of the gas turbine is controlled between 0.3 and 0.74 kg/min. There are many heating demands in winter. The gas inlet velocity of the heat boiler is controlled between 0.16 and 0.48 kg/min. The heat pump's water inlet velocity is controlled between 0.14 and 0.45 m³/min. The inlet water velocity of the heat exchanger is controlled between 0.08 and 0.24 m³/min. Meanwhile, the gas inlet velocity of the heat exchanger is controlled between 0.08 and 0.26 kg/min. At the same time, through the system simulation results, the comprehensive energy utilization rate of the adjusted system reaches 72.63%, with a high degree of utilization.

As shown in Fig. 5.2, according to the statistics, the typical daily cooling load in summer is between 295 and 893 kW, the heating load demand is between 190 and 590 kW, and the electricity load demand is between 200 and 880 kW. The inlet rate adjustment scheme of equipment under this requirement is obtained through simulation, and the gas inlet rate of the gas turbine is controlled at 0.25–0.68 kg/min. There is a great demand for cooling load in summer. The gas inlet velocity of the lithium bromide refrigerator is controlled between 0.08 and 0.28 kg/min, and the water inlet velocity of the lithium bromide refrigerator is maintained between 0.06 and 0.25 m³/min. The specific scheme is shown in the figure. At the same time, the total energy utilization rate of typical summer days is 75.69% after simulation, and the efficiency is considerable.

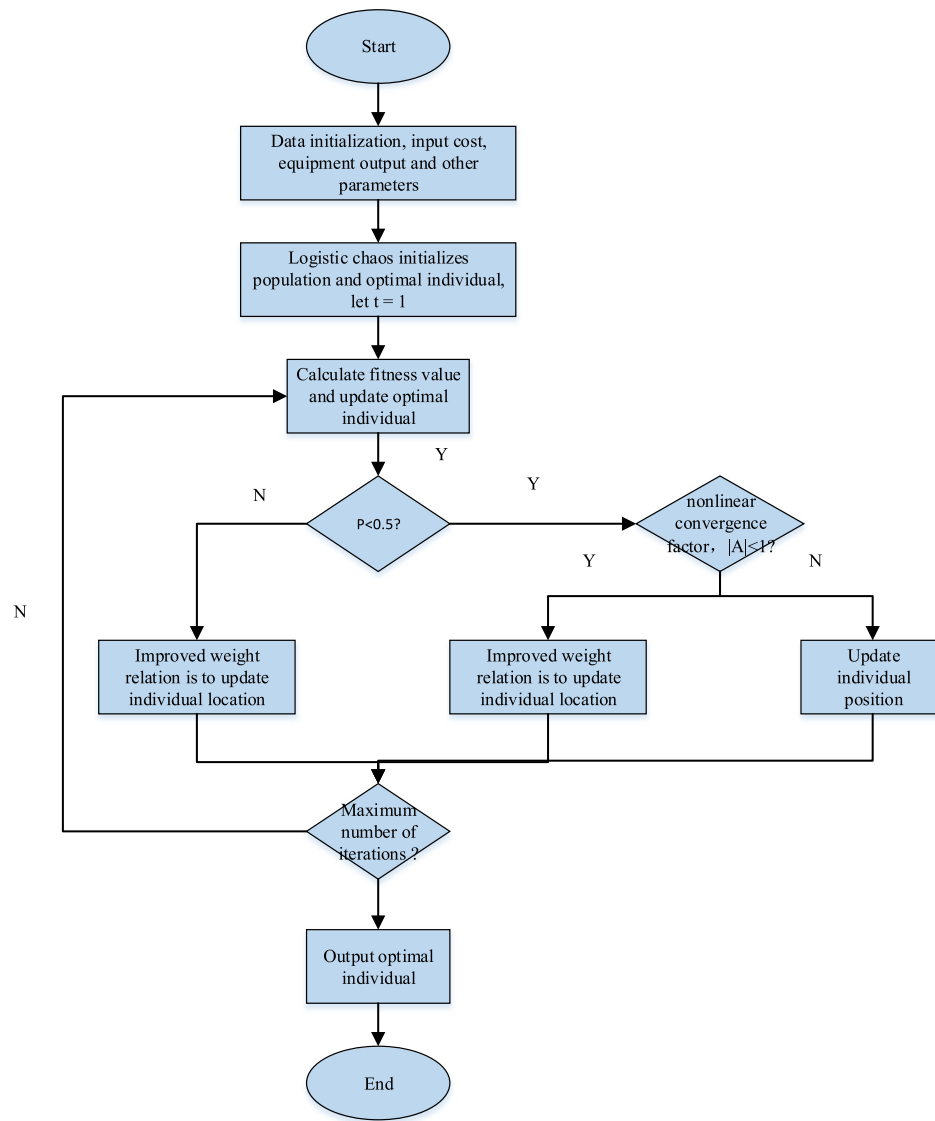


Fig. 4.2.3. Flow chart of the improved whale optimization algorithm.

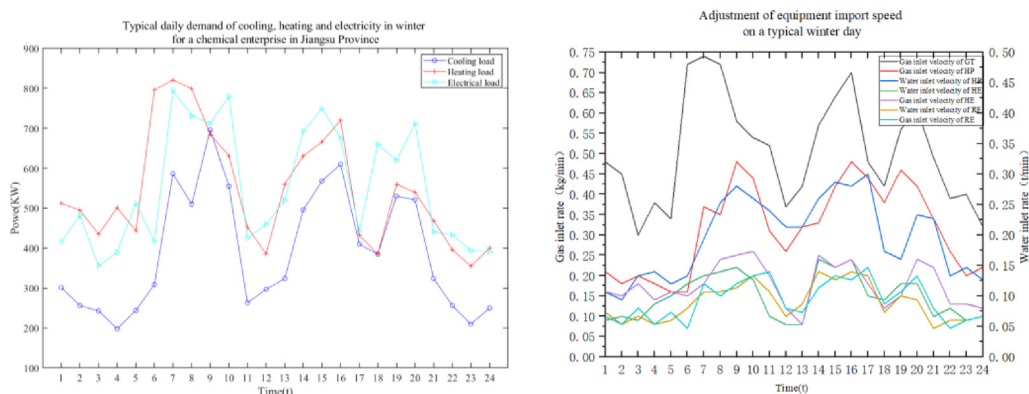


Fig. 5.1. Typical daily demand for cooling, heating, and electricity in winter of a chemical enterprise in Jiangsu Province (left figure). Rate adjustment scheme for equipment imports on a typical winter day (right figure).

It can be observed from the above adjustment scheme that the speed control scheme of each cooling, heating, and electricity generation equipment is designed according to the cooling, heating, and electricity requirements of specific salt production plants.

The purpose of preliminary energy scheduling of the system is realized. The comprehensive energy utilization rate for winter and summer shows that the adjustment scheme is better and can be applied to the system.

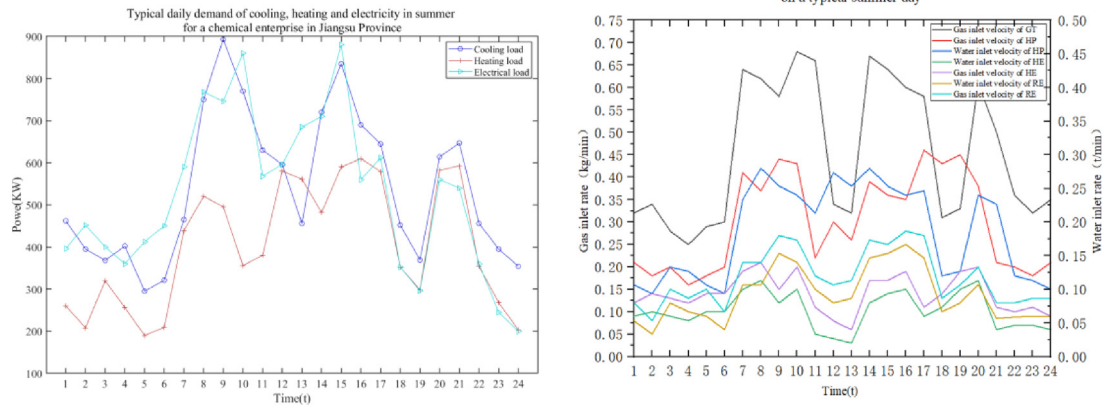


Fig. 5.2. Typical daily demand for cooling, heating, and electricity in summer of a chemical enterprise in Jiangsu Province (left figure). Rate adjustment scheme for equipment imports on a typical summer day (right figure).

Table 5.2.1 Electricity price in the Jiangsu area.

Item	Peak period	Normal period	Valley period
Time frame	8:00–12:00 17:00–21:00	12:00–17:00 21:00–24:00	0:00–8:00
Power grid purchase Price/¥ (kW h) ⁻¹	1.1141	0.6664	0.2987
Power grid sale price/¥ (kW h) ⁻¹	0.6541	0.3464	0.1872

5.2. Setting of CCHP system

5.2.1. Relevant parameter settings

The simulation model selects the gas turbine, photovoltaic generator, wind turbine, and graphene battery as the electricity supply model, heat boiler, heat pump, heat exchanger, and molten salt storage tank as the heating model, and lithium bromide refrigerator and electric refrigerator as the cooling model. Taking the cooling, heating, and electricity supply of a salt plant in Jiangsu Province as an example, the calculation cycle is 24 h, and the improved whale optimization algorithm is adopted. The parameters are set as follows: the population size (N) is 100, and the iteration number is 500. The model uses industrial electricity prices in Jiangsu Province, as shown in Table 5.2.1. The equipment maintenance cost parameters for each of equipment in the system are shown in Table 5.2.2. The equipment investment cost parameters for CCHP unit are shown in Table 5.2.3. Treatment costs for emissions of gases (CO₂, SO₂, NO_x) and emission parameters for each equipment in a region of Jiangsu are used, as shown in Table 5.2.4. Use the wastewater discharge grade of a certain area in Jiangsu Province and the treatment cost for the discharged wastewater, as shown in Table 5.2.5.

5.2.2. Wind and solar power

In this paper, the system is designed to obtain the optimal energy scheduling scheme of the system by inputting the wind-solar power of the CCHP system.

Wind and light motor electricity generation by combining actual local wind and light related influence data and equipment configuration, simulation results. Firstly, the wind speed data source of a certain area in Jiangsu comes from the NASA database. The installed capacity of the wind turbine is set to 1 MW, and the wind turbine configuration is carried out. The wind generation in Jiangsu is simulated, and the electrical power of the wind turbine is obtained, as shown in Fig. 5.2.2. Finally, PVSYST is used to simulate the photovoltaic operation. And the photovoltaic

Table 5.2.2 Equipment maintenance cost parameters.

Class of device	The upper limit of equipment power (kW)	Maintenance cost (¥/kWh)
Gas turbine	1000	0.03
Gas boiler	500	0.021
Heat pump	500	0.025
Heat exchanger	500	0.016
Lithium bromide refrigerator	500	0.032
Electric refrigerator	300	0.015
Photovoltaic generator	500	0.02
Wind generator	500	0.02
Graphene battery	500	0.056
Water storage tank	500	0.018
Molten salt heat storage tank	500	0.026

Table 5.2.3 Equipment investment cost parameters.

Unit name	Service life (year)	Investment cost (¥)
CCHP unit	15	1000000

battery capacity is set to 0.5 MW. The configuration of photovoltaic modules, inverters, and arrays is designed. Combined with the regional meteorological data (solar radiation), the simulation is carried out to obtain the photovoltaic power, as shown in Fig. 5.2.3.

As shown in the figure above, the typical winter day in a region of Jiangsu can generate 88.93–497.73 kW at wind speeds of 6.22–11.65 m/s. On a typical summer day, the wind speed of 5.47–8.11 m/s can generate 107–358 kW directly. Visible, the region is rich in wind resources and more wind power in winter.

The above figure shows that the typical winter days in a region of Jiangsu are between 7:00 and 17:00. Horizontal solar radiation is 157.7–891.9 W/m², generating 46–306 kW. This area's typical summer sunshine is from 6:00 to 20:00. Horizontal solar radiation ranges from 43 to 791.9 W/m² and electricity generation ranges from 10 to 306 kW. It can be seen that the photovoltaic resources in this region are abundant, and there is abundant solar energy in winter and summer.

5.3. CCHP system for absorption of chemical waste heating

The CCHP system proposed in this paper has good adaptability to chemical enterprises. A better energy scheduling scheme is obtained through the relevant parameter configuration and

Table 5.2.4
Gas control index of a region in Jiangsu Province.

Type of pollutant		CO ₂	SO ₂	NO _x
Pollution emission coefficient (g/kWh)	Gas turbine	720.5	0.0053	0.0028
	Heat pump	420.3	0.003	0.0015
	Heat exchanger	230	0.0012	0.0009
	Lithium bromide refrigerator	263	0.0028	0.0016
	Power grid	980	3.4	2.8
Treatment cost (¥/kg)		0.0074	4.9255	6.8256

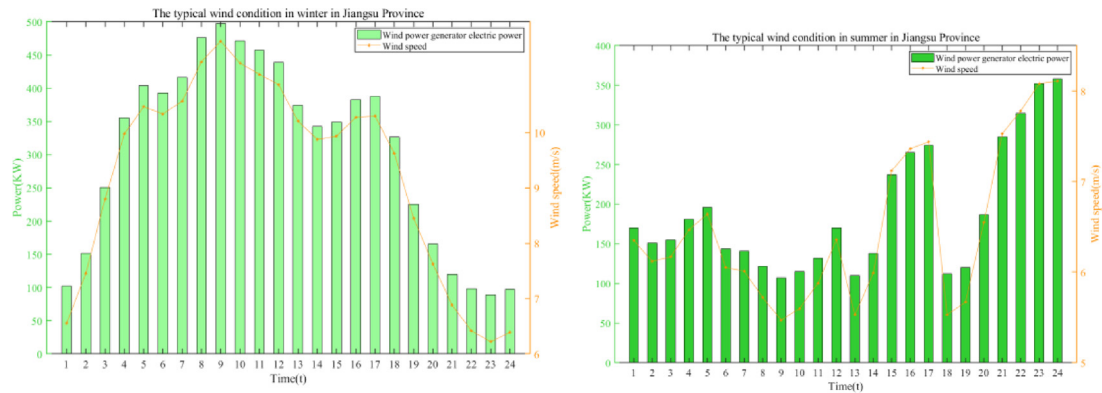


Fig. 5.2.2. The typical wind condition in winter in Jiangsu Province (left figure). The typical wind condition in summer in Jiangsu Province (left figure).

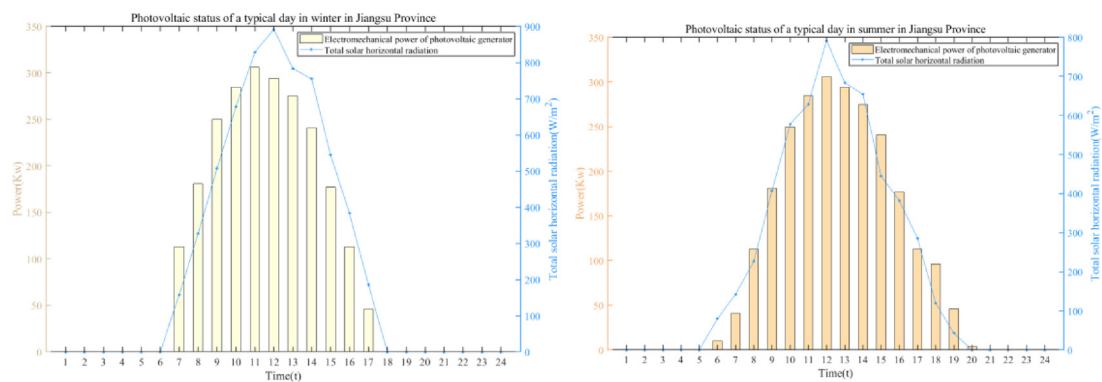


Fig. 5.2.3. Photovoltaic status of a typical day in winter in Jiangsu Province (left figure). Photovoltaic status of a typical day in summer in Jiangsu Province (right figure).

Table 5.2.5
Treatment index of chemical wastewater in Jiangsu Province.

Type of pollutant		Chemical effluent
Pollution emission coefficient (t/kWh)	Heat pump	2.35
	Heat exchanger	1.32
	Lithium bromide refrigerator	0.98
Treatment cost (¥/t)		3.84

scheduling strategy configuration, and the improved whale optimization algorithm to optimize the comprehensive cost. The simulation diagram of the CCHP system for absorbing chemical waste heating is as follows. Fig. 5.3.1 is the optimal scheduling of a typical cooling network for the CCHP system absorbing chemical waste heating in winter and summer. Fig. 5.3.2 is the optimal scheduling of a typical heating network for the CCHP system absorbing chemical waste heating in winter and summer. Fig. 5.3.3 is the optimal scheduling of a typical electricity network for the CCHP system absorbing chemical waste heating in winter and summer. Fig. 5.3.4 shows the comprehensive cost comparison of typical winter and summer days of the algorithm optimization system before and after improvement. Table 5.3.1 is the cost

comparison of the before and after improved whale optimization algorithm system on a typical winter day. Table 5.3.2 is the cost comparison of the before and after improved whale optimization algorithm system on a typical winter day.

It can be seen from Figs. 5.3.1, 5.3.2, and 5.3.3 that under the equipment energy scheduling strategy and the improved whale optimization algorithm, the CCHP system with chemical waste heating absorption realizes the full utilization of cooling, heating, and electricity. According to the specific load demand of the salt plant, the corresponding energy optimization scheduling is realized. Under the premise of meeting the needs of salt plants, it can realize the scheduling of cooling, heating, and electricity, especially in the power grid, and realize the reasonable purchase and sale of electricity. It improves the comprehensive utilization rate of system energy, avoids excessive energy waste, and reduces the comprehensive cost.

In terms of the cooling network, according to the cooling demand curve of the salt plant, the classification regulation of the electric and lithium bromide refrigerators is realized through the load scheduling strategy. Lithium bromide refrigerator output power is 16–146 kW and 32–145 kW. The lithium bromide refrigerator in the cooling-net equipment provides an average cooling

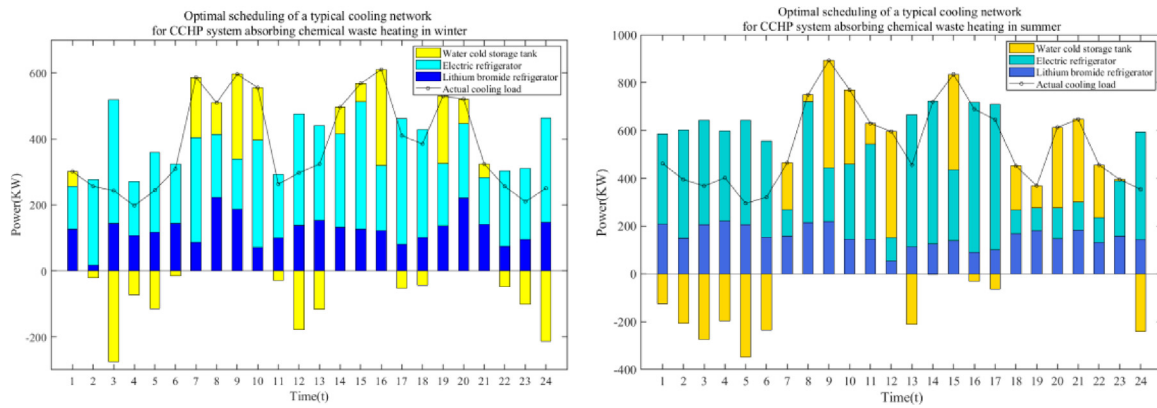


Fig. 5.3.1. Optimal scheduling of a typical cooling network for CCHP system absorbing chemical waste heating in winter (left figure). Optimal scheduling of a typical cooling network for CCHP system absorbing chemical waste heating in summer (right figure).

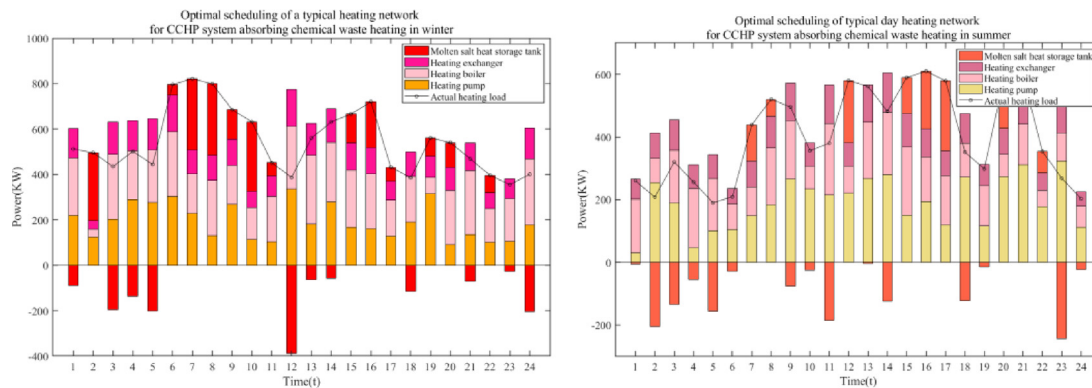


Fig. 5.3.2. Optimal scheduling of a typical heating network for CCHP system absorbing chemical waste heating in winter (left figure). Optimal scheduling of a typical heating network for CCHP system absorbing chemical waste heating in summer (right figure).

load of 6.25–58.4% and 7.01–16.64% in winter and summer. After optimizing the improved whale optimization algorithm, the cooling storage is realized when the cooling demand is low, and the release is carried out at the cooling demand's peak, relieving the system pressure and avoiding the waste phenomenon when the cooling load is sufficient.

It can be seen from the figure that the demand for cooling load in the salt plant increased significantly in summer, mainly through the efficient operation of electric refrigerators to improve the supply of cooling load.

The energy scheduling strategy realizes the heating network's classification regulation of the boilers, heat pumps, and heat exchangers. The improved whale optimization algorithm optimizes the heating network. The heating demand is reduced at night, and at noon, the heating load is stored and released during the peak period of heating demand. It relieves the supply pressure of the heat pump, boiler, and heat exchanger. Reduce the system's economic operation cost and complete the heating network's energy scheduling. It can be seen from the two figures that the demand for heating in winter is increased, and there is more heating production equipment that can supply the heating load required by the enterprise. Heat pump output power is 90–336 kW and 30–322 kW in winter and summer. The abundant water heating is recycled, which increases the channels provided by the system heating and provides 15.4–57.9% and 11.5–62.9% of the heating load of the heating network in winter and summer.

The gas turbine is adjusted through the energy scheduling strategy to realize the electric load's main supply in the power grid. Secondly, the improved whale optimization algorithm further optimizes the energy scheduling process so that purchasing

and selling electricity, wind electricity, photovoltaic electricity generation, and graphene batteries can achieve efficient load supply in the most economical time. Wind and photovoltaic generation provide 0%–30% of the electric load of the electricity network. It can be seen from the two figures that the region has more wind and solar power in winter, so the winter electricity scheduling is also sufficient, and the electricity is more redundant and sold. Due to the increase in electricity consumption in summer, it is necessary to purchase electricity to meet energy demand.

Fig. 5.3.4 shows that the improved whale optimization algorithm converges in 17 generations in winter and 137 generations in summer. Faster than 193 generations of typical winter days and 183 generations of a typical summer day before improvement. The cost of the improved whale optimization algorithm is reduced by ¥ 870 on a typical winter day and ¥ 690 on a typical summer day. Therefore, the improved whale optimization algorithm is superior to the basic whale optimization algorithm in convergence speed and optimization accuracy. The comprehensive cost of the CCHP system absorbing chemical waste heating is further reduced, and a better scheduling scheme is obtained.

On a typical winter day, Table 5.3.1 shows that the comprehensive cost of the improved whale optimization algorithm is ¥ 35 312, better than that of the basic whale optimization algorithm. Compared with the latter, the comprehensive cost is reduced by 2.4% and has been greatly improved.

The cost of natural gas and electricity purchase and sale are reduced by 19.42% and 23.95%, respectively, due to the optimal scheduling and the rational use of system energy. It can also improve the electricity sale in the redundant stage of system energy, and the optimization effect is excellent.

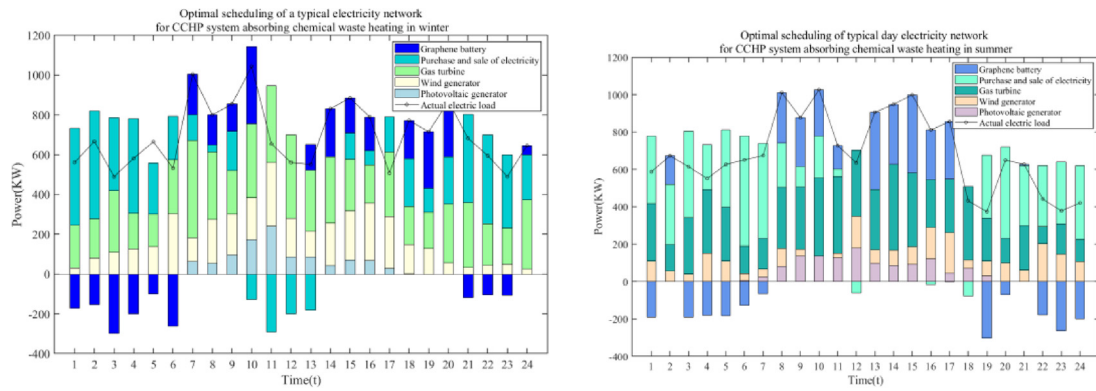


Fig. 5.3.3. Optimal scheduling of a typical electricity network for CCHP system absorbing chemical waste heating in winter (left figure). Optimal scheduling of a typical electricity network for CCHP system absorbing chemical waste heating in summer (right figure).

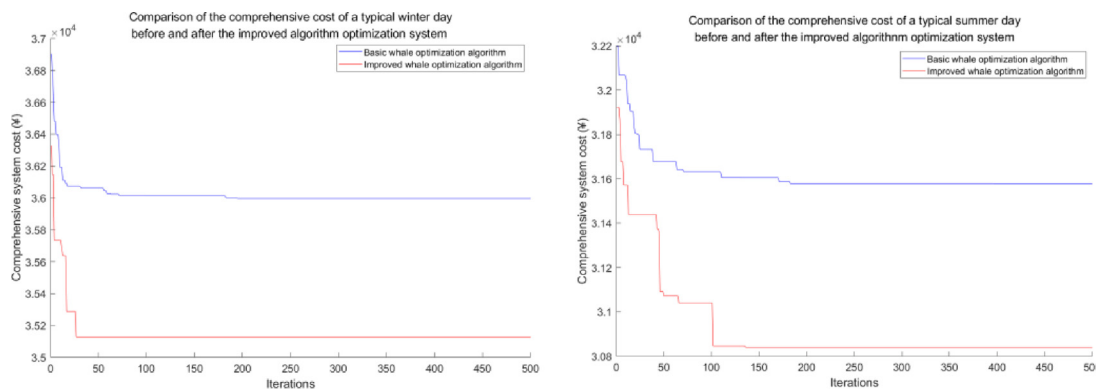


Fig. 5.3.4. Comparison of the comprehensive cost of a typical winter day before and after the improved algorithm optimization system (left figure). Comparison of the comprehensive cost of a typical summer day before and after the improved algorithm optimization system (right figure).

Table 5.3.1

Cost comparison of whale optimization algorithm system before and after improvement on a typical winter day.

Cost types	Cost of basic whale optimization algorithm (¥)	Cost of improved whale optimization algorithm (¥)	Comparison (%)
Resultant costs	36 182	35 312	−2.40
Equipment maintenance and investment cost	1492	1548	+3.75
Gas cost	4983	4015	−19.42
Electricity purchase and sale cost	2230	1696	−23.95
Environmental governance cost	27 477	28 053	+2.1

Table 5.3.2

Cost comparison of whale optimization algorithm system before and after improvement on a typical winter day.

Cost types	Cost of basic whale optimization algorithm (¥)	Cost of improved whale optimization algorithm (¥)	Comparison (%)
Resultant costs	31 752	31 062	−2.17
Equipment maintenance and investment cost	1610	1620	+0.62
Gas cost	4886	4703	−3.75
Electricity purchase and sale cost	4862	3227	−33.63
Environmental governance cost	20 394	21 512	+0.55

On a typical summer day, Table 5.3.2 shows that the comprehensive cost of the improved whale optimization algorithm is ¥ 31 062 better than that of the basic whale algorithm, and the comprehensive cost is reduced by 2.17%, with more improvement.

The demand for cooling load is great on typical days in summer, and the system regulates the refrigeration equipment. Therefore, the electricity consumption is also higher than that on typical days in winter. And the demand for natural gas is also rising.

The comprehensive cost is still better than the basic whale optimization algorithm. Due to the influence of power grid scheduling, the improved whale algorithm reduces the purchase and sale of electricity by 33.63% and the cost of natural gas by 3.75%, indicating the rationality of the optimization scheduling strategy.

Therefore, the optimized scheduling results of the improved whale optimization algorithm for the CCHP system that absorbs chemical waste heating align with expectations. The results are better than those of the basic whale algorithm. In winter and

summer, typical days can complete the chemical enterprise energy supply with lower comprehensive cost.

6. Conclusion

In this paper, aiming to supply multiple energy for a chemical enterprise in Jiangsu Province, a new structure of the CCHP system is designed. This paper collects the load demand data of a salt factory in Jiangsu Province and optimizes system operation and optimal cost management. In this paper, the improved whale optimization algorithm is used to optimize the control of the CCHP system. Finally, the main research results are as follows:

1. By connecting the heat pump to the CCHP system, 20–35t of wastewater discharged by chemical enterprises can be recycled daily. The abundant water heating is recycled, which increases the channels provided by the system heating and provides 15.4–57.9% and 11.5–62.9% of the heating load of the heating network in winter and summer.

2. The thermal cascade recovery system is designed by heat pump/heat exchanger-lithium bromide refrigerator. The high-temperature gas discharged by the system and the heating in the external recycled chemical wastewater are recycled step by step. The lithium bromide refrigerator in the cooling-net equipment provides an average cooling load of 6.25–58.4% and 7.01–16.64% in winter and summer. The visible heating recovery part of the energy is still considerable and effective.

3. Combining the design of cooling, heating, and electricity three kinds of energy storage equipment and a CCHP system. In the process of energy scheduling, the load redundancy and energy charging and discharging at an insufficient time are realized. The energy storage units are set through simulation experiments - 500–500 kW, which plays an important role in the system energy scheduling process.

4. In terms of operation strategy, the design of equipment classification adjustment is used to realize the control of the load flow of cooling, heating, and electricity by adjusting the inlet water velocity and inlet gas velocity of the input ports of gas turbine, heat boiler, heat pump, electric refrigerator, and lithium bromide refrigerator.

5. The wind-solar complementary new energy electricity supply equipment connects the wind turbine and photovoltaic generator to the CCHP system proposed in this paper. Through software simulation, the local wind speed in Jiangsu in winter and summer can reach 5.5–12 m/s, and the solar horizontal radiation can reach 0–900 W/m². The two can provide 0%–30% of the electricity, which greatly reduces the excessive dependence of the system on gas turbines. It is suggested that this part of the equipment should be located in the open ground area to realize the effective use of new energy.

6. Using the improved whale optimization algorithm to optimize the scheduling and absorption of chemical waste heating CCHP system and compare the two. From the perspective of comprehensive cost, the improved whale optimization algorithm reduces the cost of typical winter and summer days by 2.4% and 2.17%, respectively. The system cost saved in the long run is very considerable, which greatly reduces the use cost of the system. From the cost rules, mainly after the optimal scheduling, the cost of electricity purchase and sale and the cost of natural gas are reduced. The cost of natural gas in winter and summer is reduced by 19.42% and 3.75%, respectively. And the cost of electricity purchase and sale in winter and summer is reduced by 23.95% and 33.63%, respectively. It can be seen that the improved whale optimization algorithm has an obvious optimization scheduling effect on the CCHP system that absorbs chemical waste heating and can be applied to the actual chemical plant.

This paper presents the method of optimizing the scheduling of CCHP system. It not only solves the waste problem of chemical wastewater, but also improves the energy utilization rate of chemical enterprises. The CCHP system is used to provide multi energy for chemical enterprises, and the system energy is reasonably optimized for scheduling, which reduces the comprehensive cost of chemical enterprises.

However, this method is only applicable to wastewater discharged in the exothermic process of chemical reaction. In the future, other forms of waste heat in chemical enterprises can be considered. Or make structural improvement of CCHP to make it more widely applicable.

CRedit authorship contribution statement

Jie Ji: Conceptualization, Methodology, Writing – original draft. **Jingxin Qin:** Data curation, Writing – original draft. **Rundong Ji:** Methodology, Software. **Hui Huang:** Visualization, Investigation. **Fucheng Wang:** Software, Validation. **Muhammad Shahzad Nazir:** Software, Validation. **Mengxiong Zhou:** Writing – review & editing. **Yaodong Wang:** Supervision.

Declaration of competing interest

The authors declare that they have no known competing financial interests or personal relationships that could have appeared to influence the work reported in this paper.

Data availability

Data will be made available on request.

References

- Ahmed, T., Raha, I.T., Safwat, F., et al., 2021. Impact of message size on least significant bit and chaotic logistic mapping steganographic technique. 5(4) 1100–1104.
- Ai, T., Chen, H., Jia, J., et al., 2022. Thermodynamic analysis of a CCHP system integrated with a regenerative organic flash cycle. *Appl. Therm. Eng.* 202, 117833.
- Cheng, Z., Jia, D., Li, Z., et al., 2022. Multi-time scale dynamic robust optimal scheduling of CCHP microgrid based on rolling optimization. *Int. J. Electr. Power Energy Syst.* 139, 107957.
- Cui, Q., Zhu, J., Chen, J., et al., 2022. Optimal operation of CCHP microgrids with multiple shiftable loads in different auxiliary heating source systems. *Energy Rep.* 8, 628–638.
- Guanghua, L., 2019. Study on Structure Design and Performance Optimization of Small Capacity Molten Salt Heat Storage Device. Southeast University.
- Guian, C., Jiahui, W., Lei, Y., et al., 2022. Operation optimization of CCHP microgrid based on improved dynamic inertia weight particle swarm optimization algorithm. *Sci. Technol. Eng.* 22 (04), 1472–1479.
- Hui, L., You, W., Xiangjie, X., et al., 2021. Parameter identification of transmission chain of DFIG based on improved PSO. 42(12) 9.
- Jianmin, H., Zhihao, X., Weijie, Y., et al., 2022. Hybrid load following operation strategy of building triple supply system considering energy storage characteristics. *Electr. Power Construct.* 43 (05), 50–62.
- Jiaxiu, Z., Luning, W., Xuejie, L., et al., 2022. Simulation research on gas turbine CCHP system under different operation modes. *J. Qingdao Technol. Univ.* 42 (01), 58–65.
- Jiazheng, W., Guoyuan, M., Guoxin, Y., et al., 2022. Experimental study on domestic air source heat pump water heater with flash air supply. *J. Refrig.* 07 (04), 1–9.
- Keskin, I., Soykan, G., 2022. Optimal cost management of the CCHP based data center with district heating and district cooling integration in the presence of different energy tariffs. *Energy Convers. Manage.* 254, 115211.
- L, J., 2021. Whale optimization algorithm based on multi-population bidirectional learning and information exchange. *J. Electron. Inform.* 43 (11), 10.
- Leitian, C., Hang, Y., 2018. Application of temperature stratified water thermal storage device in SAIC Volkswagen. *Shanghai Energy Conserv.* (01), 56–61.
- Li, Y., Tian, R., Wei, M., 2022. Operation strategy for interactive CCHP system based on energy complementary characteristics of diverse operation strategies. *Appl. Energy* 310, 118415.
- Liang, S., Jiawen, L., Xinhe, Y., et al., 2021. Multi-objective optimal configuration of combined cooling, heating and power microgrid with phase change energy storage. 41(10) 7.

- Liang, W., Lin, S., Lei, S., et al., 2022. Distributionally robust optimal dispatch of CCHP campus microgrids considering the time-delay of pipelines and the uncertainty of renewable energy. *Energy* 239, 122200.
- Linlin, J., Qinrong, L., 2020. Research on development status of CCHP system. *Sci. Technol.* (16), 171+182.
- Lu, Z., Duan, L., Wang, Z., 2022. Performance evaluation of a novel CCHP system integrated with MCFC, ISCC and LiBr refrigeration system. *Int. J. Hydrogen Energy* 47 (48), 20957–20972.
- Meijin, L., 2021. Grey wolf optimization algorithm based on improved convergence factor and mutation strategy. *J. Foshan Univ. Sci. Technol. Nat. Sci. Ed.*
- Mingzhe, Q., Yi, Z., Tianxing, S., 2022. Design of sewage source heat pump system for an office building of a sewage treatment plant. *Technol. Innov. Appl.* 12 (18), 96–99.
- Mirjalili, S., Lewis, A., 2016. The whale optimization algorithm. *Adv. Eng. Softw.* 95, 51–67.
- Shouyang, L., 2022. Production technology and optimization of titanium dioxide CCHP. *Contemp. Chem. Res.* (04), 171–173.
- Tooryan, F., Hassanzadehfard, H., Dargahi, V., et al., 2022. A cost-effective approach for optimal energy management of a hybrid CCHP microgrid with different hydrogen production considering load growth analysis. *Int. J. Hydrogen Energy* 47 (10), 6569–6585.
- Xinrou, B., 2022. Optimal Dispatching Strategy of Regional Integrated Energy System Based on a Cooling, Heating, and Power Combined Industrial Park. Chongqing University of Technology, 000438.
- Xu, Y., Luo, X., Tu, Z., 2022. 4E analysis of a SOFC-CCHP system with a LiBr absorption chiller. *Energy Rep.* 8, 5284–5295.
- Xuntao, G., Gaoyan, H., 2020. Overview of modeling methods for CCHP system. *Zhejiang Electr. Power* 39 (4), 11.
- Yang, Z., Bing, L., Wen, L., et al., 2022. Nonlinear optimal scheduling method for combined cooling, heating and power system considering ice storage. *Energy Conserv.* 41 (05), 47–52.
- Yin, C., 2021. The dilemma of alternating old and new energy. *Legal Person* (10), 56–58.
- Yuanyuan, F., Yubo, Y., Runjie, B., et al., 2022. Controllable standby VO₂/GO composite and its application in water system zinc ion battery. *Changshu Inst. Technol.* 36 (05), 16–20.
- Zhang, Y., Zhao, H., Li, B., et al., 2022. Research on dynamic pricing and operation optimization strategy of integrated energy system based on stackelberg game. *Int. J. Electr. Power Energy Syst.* 143, 108446.
- Zhuohan, J., Zhigang, L., Jiazhu, X., et al., 2021. A bi-level collaborative optimization configuration method for combined cooling, heating and power system considering wind and solar storage. *Electr. Power Construct.* 42 (08), 71–80.